Vol. 615: 177–188, 2019
https://doi.org/10.3354/meps12926
MARINE ECOLOGY PROGRESS SERIES
Mar Ecol Prog Ser
Published April 18

Estimating the density of resident coastal fish using underwater cameras: accounting for individual detectability

Guillermo Follana-Berná[1,2,3,*], Miquel Palmer[3], Andrea Campos-Candela[3,4], Pablo Arechavala-Lopez[3], Carlos Diaz-Gil[1,2,3], Josep Alós[3], Ignacio A. Catalan[3], Salvador Balle[3], Josep Coll[5], Gabriel Morey[5], Francisco Verger[5], Amalia Grau[1,2]

[1]Laboratori d'Investigacions Marines i Aqüicultura, LIMIA (Balearic Government), 07157 Port d'Andratx, Illes Balears, Spain
[2]Instituto de Investigaciones Agroambientales y de Economía del Agua, INAGEA (INIA_Govern Balear-UIB), 07122 Palma, Illes Balears, Spain
[3]Fish Ecology Lab, Instituto Mediterráneo de Estudios Avanzados, IMEDEA (CSIC-UIB), 07190 Esporles, Illes Balears, Spain
[4]Department of Marine Sciences and Applied Biology, University of Alicante, 03080 Alicante, Spain
[5]Tragsatec, 07009 Palma, Illes Balears, Spain

ABSTRACT: Technological advances in underwater video recording are providing novel opportunities for monitoring wild fish. Although extracting data from videos is often challenging, accurate and precise estimates of density for animals whose normal activities are restricted to a bounded area or home range can be obtained from counts averaged across a relatively low number of video frames. However, this method requires that individual detectability (P_{ID}, the probability of detecting a given animal provided that it is actually within the area surveyed by a camera) be known. Here we propose a Bayesian implementation for estimating P_{ID} after combining counts from cameras with counts from any other reference method. The proposed framework was demonstrated with a case study of *Serranus scriba*, a widely distributed and resident coastal fish. Density and P_{ID} were calculated after combining fish counts from unbaited remote underwater video (RUV) and underwater visual censuses (UVC) as reference methods. The relevance of the proposed framework is that after estimating P_{ID}, fish density can be estimated accurately and precisely at the UVC scale (or at the scale of the preferred reference method) using RUV only. This method is further validated using computer simulations based on empirical data. We provide a simulation tool kit for comparing the expected precision attainable for different sampling effort and for species with different levels of P_{ID}. Overall, the proposed method may contribute to substantially enlarge the spatio-temporal scope of density monitoring programmes for many resident fish.

KEY WORDS: Bayesian approach · Fish density · Home range · Individual detectability · Monitoring · Unbaited underwater cameras · Underwater visual census

1. INTRODUCTION

One of the fundamental challenges in marine ecology and fisheries science is to describe the current state of fish populations in terms of abundance, which is imperative for understanding population dynamics (Hilborn & Walters 1992, Agnew et al. 2013). However, reliable abundance data at relevant spatio-temporal scales are rarely available in marine systems. Data scarcity is especially severe in the cases of recreational and artisanal fisheries targeting resident coastal fish, for which science-based, sustainable management tends to be unfeasible (Pita et al. 2018). In addition, even in well-monitored fish-

*Corresponding author: gfollana@dgpesca.caib.es

eries, most of the data come from catches. However, the usefulness of fisheries-dependent data (e.g. captures per unit effort, CPUE) as a proxy of abundance is under debate (Pauly et al. 2013). For example, catch-related data may be biased against the less vulnerable fish species or the less vulnerable fraction within a given species (Alós et al. 2014, 2015, 2018). Further, the behaviour of both fish and fishermen may induce a lack of proportionality between CPUE and fish density, producing hyperdepletion or hyperstability (Lennox et al. 2017).

The existence of bias when estimating abundance is widely recognized for both fishery-dependent and -independent methods. Among fishery-independent methods (Murphy & Jenkins 2010, Mallet & Pelletier 2014, Przeslawski & Foster 2018), divers counting fish along standardized transects (i.e. underwater visual census, UVC) or point counts have been so widely used for monitoring many coastal fish species (Murphy & Jenkins 2010) that they currently represent standard reference methods. UVC is a non-destructive method with many advantages, but it suffers from some well-known drawbacks. Biases may occur due to different behavioural responsiveness of fish species to the presence of divers (Lindfield et al. 2014), observer-related effects (Dickens et al. 2011) or within-transect variability (Kulbicki et al. 2010). Most of these problems are currently dealt with by using highly standardized protocols, because biases are assumed to be consistent for a given species, thus allowing between-study comparisons (Ackerman & Bellwood 2000, Ward-Paige et al. 2010). One of the main concerns about UVC is the large investment in time and personal effort needed. The immediate outcome is that sample sizes tend to be small both at temporal and at spatial scales (Thompson & Mapstone 1997). Although reduced sample sizes do not necessarily introduce bias, they do imply worse precision and wider confidence intervals.

In contrast, the use of underwater cameras or action cameras is experiencing an increased interest because cameras allow long-term, high-frequency monitoring of fish and marine environments (Assis et al. 2013, Aguzzi et al. 2015, Easton et al. 2015), with the added value of avoiding any diver-related bias. The main advances that promote the use of cameras are miniaturization, decreased cost, shock proofing, water proofing over a wide depth range, long-life batteries, high-capacity memory cards and high-definition images (Struthers et al. 2015). Additional potential applications of remote underwater video cameras (RUVs) include their usefulness in marine reserves or for monitoring endangered species (Murphy & Jenkins 2010). In addition, RUVs can cover broader spatial and temporal scales (Pelletier et al. 2012, Assis et al. 2013), and potential biases due to the physical environment or to behavioural and life history characteristics might also be reduced.

However, RUV recordings have some disadvantages, including a limited field of vision, the need for good visibility and the cost related to image processing (Pita et al. 2014, Struthers et al. 2015). In most cases, bait is used to attract fish to the camera (Whitmarsh et al. 2017). Several problems preclude any reliable estimation of absolute density using baited cameras (Whitmarsh et al. 2017), including the unknown dynamics of the bait odour plume, how such dynamics affect attractiveness (Dunlop et al. 2015), how the fish already attracted by the bait are themselves a visual cue for other fish, and the plausible existence of species-specific responses and internal state dependence of individual fish. Instead, several relative abundance metrics have been proposed; two of the most popular metrics are MaxN and MeanCount (Stobart et al. 2007, 2015, Schobernd et al. 2014, Campbell et al. 2015). These metrics have been developed because most ecologists and managers have concerns about counting the same individual more than once (Ward-Paige et al. 2010, Assis et al. 2013, Campbell et al. 2015).

Along with the technological opportunities offered by camera-based wildlife assessment, it was recently demonstrated that fish density (number of animals per unit area) can be properly estimated from fish counts across relatively few video frames obtained with an unbaited camera (Campos-Candela et al. 2018). One of the key assumptions of this proposed method is that animal density does not change at the spatial and temporal scale of a given RUV sample. This assumption is met by many resident coastal fish that generally remain within a given area of activity, or home range (HR), which tends to be orders of magnitude smaller than the extent of suitable habitat (March et al. 2010, Villegas-Ríos et al. 2014, Alós et al. 2016). For fish with HRs, no emigration, no immigration, no changes in the HR location, no birth and no death can be safely assumed at the spatial and temporal scales commonly used for sampling abundance.

Moreover, an additional assumption of the previously mentioned method is that individual detectability (probability of individual detection, P_{ID}) must be known (Campos-Candela et al. 2018). Here we define P_{ID} as the probability of counting a given fish that is actually within the area sampled by a camera. Conspicuous species are more easily detected than cryptic species (Boulinier et al. 1998), and even the same individual will be more detectable in bare habitats than in complex habitats where fish may be hidden behind rocks or within seagrass patches. Moreover, the existence of a positive relationship between detectability and density can artificially inflate between-survey heterogeneity (Dorazio & Royle 2005). Hence, the development of a method accounting for imperfect detection is indispensable for making unbiased inferences on fish density when using RUVs (Bacheler et al. 2017). Note that P_{ID} should not be confused with the concept of detectability used in ecology and conservation biology to infer whether a species inhabits a given site even when it has not been detected there (Boulinier et al. 1998, Bayley & Peterson 2001).

Here we propose and demonstrate a method for the concurrent estimation of density and P_{ID} for species (1) that display HR behaviour, (2) for which UVC represents a reliable reference method and (3) for which unbaited RUVs are a feasible alternative (Campos-Candela et al. 2018). The relevance of the method proposed here relies on the fact that after estimating P_{ID}, RUV can be used alone for producing low-cost abundance estimates at the scale of the reference method (in this case, UVC), which may entail a paradigm shift for monitoring fish density at large spatial and temporal scales. To demonstrate the method, we selected an HR-behaving serranid, *Serranus scriba*, as a case study. Accuracy and precision of the method were evaluated using computer simulation experiments (i.e. moving virtual fish according to a reliable movement model; March et al. 2010, Alós et al. 2016). Simulations were realistic in terms of fish movement, feasible fish densities and diverse P_{ID}. Finally, we provide a simulation tool for exploring the precision attainable with different sampling effort and with different P_{ID}. This tool can be used to optimize sampling strategies in the field.

2. MATERIALS AND METHODS

2.1. Theoretical framework

The logical rationale behind the method proposed herein is that fish density is the same when sampling the same site with RUV and with the reference method. Therefore, after properly adjusting for RUV detectability, RUV fish counts may provide either absolute densities when individual detectability of the reference method is perfect (i.e. all fish are detected), or density estimates at the scale of the reference method.

Under the assumptions that (1) animals move independently from one another, and (2) density is stationary at the temporal and spatial sampling scale (Campos-Candela et al. 2018), the counts obtained with the reference method (N_{REF}) are expected to be Poisson-distributed:

$$N_{REF} \sim \text{Poisson}(\lambda_{REF}) \tag{1}$$

where λ_{REF} is given by:

$$\lambda_{REF} = P_{ID.REF} D Z_{REF} = D_{REF} Z_{REF} \tag{2}$$

where $P_{ID.REF}$ is the individual detectability of the reference method, D is the (true) animal density (animals per unit area), and Z_{REF} is the area sampled with the reference method. Therefore, D_{REF} is the (relative) density at the scale of reference method after accounting for $P_{ID.REF}$.

Similarly, the counts obtained with RUV are expected to be Poisson-distributed:

$$N_{RUV} \sim \text{Poisson}(\lambda_{RUV}) \tag{3}$$

where λ_{RUV} is given by:

$$\lambda_{RUV} = P_{ID} D Z_{RUV} = \frac{P_{ID.RUV}}{P_{ID.REF}} D_{REF} Z_{RUV} = P_{ID} D_{REF} Z_{RUV} \tag{4}$$

where $P_{ID.RUV}$ is the RUV detectability relative to the P_{ID} of the reference method ($P_{ID.REF}$). Therefore, after estimating P_{ID}, fish density at the scale of the reference method can be estimated using RUV only. Note that if $P_{ID.REF} = 1$ (all fish are detected by the reference method), then RUV counts provide an unbiased estimate of the absolute density.

2.2. Study case

To demonstrate the proposed framework, data were collected from 5 sites along the SW coast of Mallorca, Spain (Fig. 1), where 51 UVCs were completed and 13 RUVs were deployed (Table S1 in the Supplement, www.int-res.com/articles/suppl/m615p177_supp.pdf). UVCs were conducted by 3 different scuba divers, between 5 and 25 m depth and between 9:00 and 12:00 h GTM, covering an area of 250 m^2 (50 m long and 5 m wide) during 25 min. Each diver completed a maximum of 4 transects d^{-1} at different sites (Table S1). Nine UVCs were completed per site, excepting 1 site where 15 UVCs were completed. Transects were located at least 20 m apart to minimize spatial autocorrelation (Ordines et al. 2005). The number of *Serranus scriba* observed during each UVC was recorded. Note that UVCs were specifically optimized for counting only *S. scriba*.

Each RUV device was a stainless steel structure equipped with 2 stereoscopic action cameras (Fig. S1

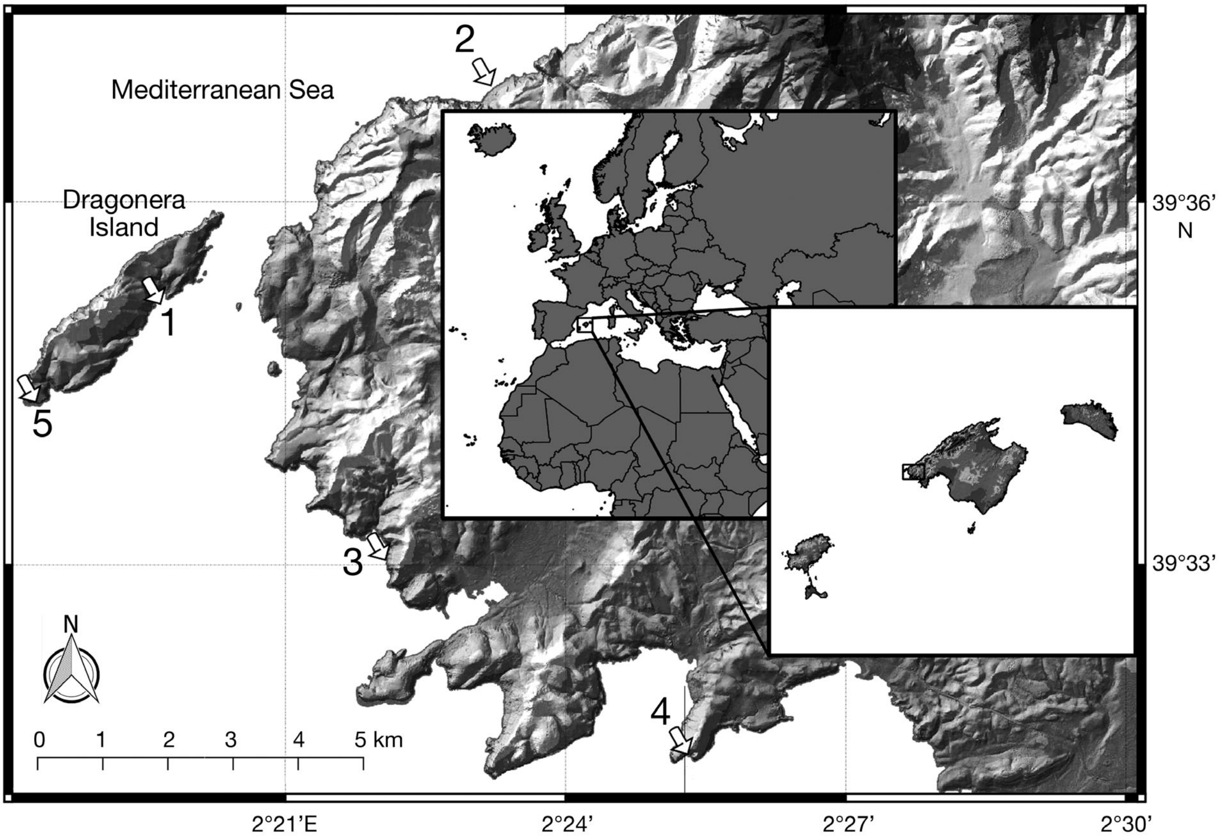

Fig. 1. Southwest coast of Mallorca Island, Spain, indicating sampling sites (white arrows); the numbers match the site numbers in Table 1 and Fig. 2. For more detail on individual sites, see Fig. S2 in the Supplement (www.int-res.com/articles/suppl/m615p177_supp.pdf)

in the Supplement). RUVs were not baited. RUV structures were deployed around the UVC locations (Fig. S2) during 4 hours (between the start of deployment at 09:00 h and the removal 14:00 h), although the maximum duration of the batteries was only approximately 3 h. Three RUVs were deployed per site; out of all the data collected, video data from 2 RUVs were discarded. Failures were caused by battery problems, poor visibility or bad deployment. Excepting those failed cases, RUVs were deployed approximately 25 m away from the corresponding UVC (for more details, see Table S1 and Fig. S2).

For video analysis, the 5 first min were excluded in order to avoid any disturbance related with the deployment itself. All individuals of *S. scriba* were counted in each frame every 150 s (or every 9000 frames). Preliminary analyses showed that this frequency minimizes temporal autocorrelation between frames. The average number of frames counted per video was 73. The distance of any given fish to the RUV was estimated using the Matlab Calibration Toolbox (Díaz-Gil et al. 2017). Fish were only counted when they were <2.5 m from the RUV. Preliminary tests suggested that at this distance, detectability did not depend on fish size. Provided that the field of view of the camera was 127°, the area surveyed was 6.93 m^2.

2.3. Modelling fish density and detectability

The UVC fish counts for a given site, diver and day ($N.UVC_{site,diver,dayUVC}$) was expected to be Poisson distributed around a mean value $\lambda.UVC_{site,diver,dayUVC}$. Site-related effect ($\mu.UVC_{site}$) was considered as a fixed factor, while diver-related effect (δ_{diver}) and *dayUVC*-related effect (δ_{dayUVC}) were considered random factors:

$$N.UVC_{site,diver,dayUVC} \sim \text{Poisson}(\lambda.UVC_{site,diver,dayUVC}) \quad (5)$$

$$\log(\lambda.UVC_{site,diver,dayUVC}) = \mu.UVC_{site} + \delta_{diver} + \delta_{dayUVC} \quad (6)$$

$$e^{\mu.UVCsite} = D_{REF} Z_{UVC} \quad (7)$$

$$\delta_{diver} \sim \text{Normal}(0,\sigma_{diver}) \quad (8)$$

$$\delta_{dayUVC} \sim \text{Normal}(0,\sigma_{dayUVC}) \quad (9)$$

where Z_{UVC} is the area of the UVC and D_{REF} is the density at the scale of the reference method in the sampled site, in this case UVC.

Concerning RUVs, the fish count for frame i at a given site, camera and day ($N.RUV_{i,site,cam,dayCAM}$) is assumed to be Poisson distributed around a mean value $\lambda.RUV_{site,cam,dayCAM}$. Site-related effect ($\mu.RUV_{site}$) was considered as a fixed factor, while camera-related effect (δ_{cam}) and *dayCAM*-related effect (δ_{dayCAM}) were considered random factors:

$$N.RUV_{i,site,cam,dayCAM} \sim \text{Poisson}(\lambda.RUV_{site,cam,dayCAM}) \quad (10)$$

$$\text{Log}(\lambda.RUV_{site,cam,dayCAM}) = \mu.RUV_{site} + \delta_{cam} + \delta_{dayCAM} \quad (11)$$

$$e^{\mu.RUVsite} = P_{ID} D_{REF} Z_{RUV} \quad (12)$$

$$\delta_{cam} \sim \text{Normal}(0,\sigma_{cam}) \quad (13)$$

$$\delta_{dayCAM} \sim \text{Normal}(0,\sigma_{dayCAM}) \quad (14)$$

where Z_{RUV} is the detection area of the camera, P_{ID} is the probability of detection, and D_{REF} is the density at the scale of the reference method in the sampled site.

The parameters of the model (Eqs. 5–14) were fitted using a Bayesian approach. Samples from the joint distribution of parameters (specifically, from D and P_{ID}), given the data (fish counts from UVC and RUV), were obtained using JAGS (http://mcmc-jags.sourceforge.net/, accessed 20 Dec 2018) (Plummer 2015) and the r2jags library (Su & Yajima 2015) of the R package (R Core Team 2017, www.r-project.org/, accessed 20 Dec 2018). Non-informative priors were assumed according to symmetric probability distributions and previously published data: a uniform prior between 0 and 1 fish m^{-2} for D (García-Charton & Pérez-Ruzafa 2001, Arechavala-López et al. 2008, Deudero et al. 2008), a uniform prior between 0 and 1 for P_{ID} and a uniform prior between 0 and 10 for the standard deviation of all random effects. Three Monte Carlo Markov chains (MCMC) were run. We drew 30 000 posterior samples. The first 15 000 iterations were discarded, and only 1 out of 10 of the remaining iterations was kept in order to prevent autocorrelation. MCMC convergence was assessed by visual inspection and evaluated using the Gelman-Rubin statistic (Plummer et al. 2006). The detailed model design, the R script and a user-friendly interface to derive the parameters for any set of data can be found at the free Shiny application website: https://fishecology.shinyapps.io/uvccam/ (accessed 20 Dec 2018).

2.4. Computer simulation experiments

The relevance of the framework proposed here is that after estimating P_{ID} with the method described in Section 2.3, fish density at new sites can be accurately and precisely estimated using RUV only. This is demonstrated here using 4 sets of simulations consisting of moving fish in a virtual scenario in which virtual cameras were deployed.

For a given simulation set, 100 replicates of 10 virtual cameras each were considered. Fish density was estimated for each replicate using the model:

$$N.RUV_{i,cam} \sim \text{Poisson}(\lambda.RUV_{cam}) \quad (15)$$

$$\text{Log}(\lambda.RUV_{cam}) = \mu.RUV + \delta_{cam} \quad (16)$$

$$e^{\mu.RUV} = P_{ID} D_{REF} Z_{RUV} \quad (17)$$

$$\delta_{cam} \sim \text{Normal}(0,\sigma_{cam}) \quad (18)$$

where P_{ID} was not estimated but was assumed to be known.

We generated movement trajectories of fish displaying HRs with the model used by Palmer et al. (2011), Alós et al. (2016) and Campos-Candela et al. (2018):

$$\vec{r}_{n+1} = \vec{r}_c + e^{-k\Delta t}(\vec{r}_n - \vec{r}_c) + \vec{R}_n \quad (19)$$

where $\vec{r}_{n+1}$ denotes the position at discrete time $t_{n+1} = (n+1)\Delta t$, $\vec{r}_n$ denotes the current position (Cartesian coordinates) of the fish at time $t_n = n\Delta t$. $\vec{r}_c$ is the position of the centre of the HR, k is a central harmonic constant force attracting the animal towards $\vec{r}_c$, and $\vec{R}_c$ is a stochastic term, normally distributed with 0 mean and standard deviation (σ in each dimension, approximated by Palmer et al. 2011):

$$\sigma = \sqrt{\frac{\varepsilon(1 - e^{-2k\Delta t})}{2k}} \quad (20)$$

The values for k (0.258 s^{-1}) and ε (631.05 m^2 s^{-1}) used for moving fish were those estimated for *S. scriba* by acoustic tracking (March et al. 2010, Campos-Candela et al. 2018). The time step Δt at which the positions of all fish were updated was set to 1 s.

Each of the 10 virtual cameras in a given replicate was set at the centre of a squared virtual scenario with each side defined as twice the radius of the HR (rHR). In the case of *S. scriba*, rHR was estimated to be 85.6 m using acoustic tracking (March et al. 2010). The rationale of using such a side length is that an animal having its centre of HR outside the scenario considered (and thus not included in the simulation) has a negligible probability of being detected by a virtual camera. The number of animals moved within such a scenario is given by side2D, where D is the fish density actually estimated for *S. scriba* (see Section 3.1). The HR centres of the virtual fish were randomly distributed within the virtual scenario.

A given virtual camera was simulated to be deployed for 10 h; thus, the number of fish movements tracked for any given fish was 360 000. However, the number of fish that were within the area surveyed by the camera was counted at 1 time step every 150 s. The number of fish counted was randomly sampled from a binomial distribution of the actual number of fish with probability defined by P_{ID}, which is assumed to be known.

The virtual simulations are designed to demonstrate the outcomes of accounting for P_{ID}. The 4 simulations differed in the value of P_{ID} considered for counting a fish ($P_{ID.sim}$) and in the way P_{ID} is modelled ($P_{ID.model}$).

Simulation 1: $P_{ID.sim}$ was set to 1 (all fish actually within the area surveyed by the camera are counted), and $P_{ID.model}$ was rightly assumed to be 1.

Simulation 2: $P_{ID.sim}$ was set to the value estimated here (P_{ID} = 0.65; see Section 3.2), but $P_{ID.model}$ was wrongly assumed to be 1 (i.e. ignoring the potential bias related to imperfect detectability).

Simulation 3: $P_{ID.sim}$ was set to 0.65, and $P_{ID.model}$ was rightly assumed to be 0.65. This set emulates the case in which P_{ID} has previously been estimated in a pilot experiment using the protocol described in Sections 2.2 and 2.3. Following this experiment, fish density is then estimated at new sites using cameras only.

Simulation 4: $P_{ID.sim}$ was set to 0.65, but the uncertainty when estimating P_{ID} was explicitly accounted for by:

$$\text{Logit}(P_{ID}) \sim \text{Normal}(\text{mean, SD}) \tag{21}$$

where mean and SD are the mean and standard deviation of the logit-transformed posterior values of the P_{ID} estimated here ($P_{ID.model}$ = 0.65, with a 95% Bayesian credibility interval between 0.34 and 0.95).

Accuracy of the estimated D in each simulation was assessed by the scaled root mean squared error (SRMSE; Walther & Moore 2005).

$$\text{SRMSE} = \frac{1}{Dr}\sqrt{\frac{1}{n}\Sigma_{j=1}^{n}(Ds_j - Dr)^2} \tag{22}$$

where Ds_j is the estimated value of density in the j^{th} simulation, and Dr is the true value. The interquantile (2.5–97.5%) range of the posterior Bayesian credibility intervals was used for assessing the precision of D.

3. RESULTS

3.1. Empirical data

Concerning the field experiments, after combining fish counts from UVC and RUV, the estimated median fish density across 5 sites ranged between 0.016 and 0.017 fish m^{-2}. Fish density appeared to be the same across sites, provided that credibility intervals largely overlapped (Fig. 2). The estimated values accounting for the different sources of variability are detailed in Table 1. Concerning P_{ID}, the 95% credibility interval ranged between 0.34 and 0.95 (median = 0.65). Thus, ignoring detectability may be a relevant concern for the species studied and with the current RUV setting.

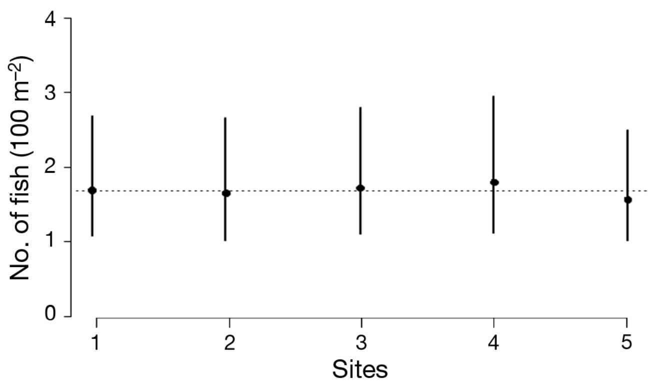

Fig. 2. Estimated fish density combining underwater visual census (UVC) and remote underwater video (RUV) with Bayesian credibility intervals (95%) at the 5 sites surveyed along the SW coast of Mallorca Island. The dotted line is the mean value of the median (50%) density of the 5 sites

Table 1. Estimated values of density (ind. 100 m^{-2}) of the 5 surveyed sites (see Fig. 1), probability of individual detection (P_{ID}) and variability of random effects (sd.cam, sd.dayCAM, sd.diver and sd.dayUVC). UVC: underwater visual census, BCI: Bayesian credibility interval, Rhat: potential scale reduction factor which explains how the chains have converged to the equilibrium distribution. Approximate convergence is diagnosed when the upper limit is close to 1

	BCI 2.5%	Median	BCI 97.5%	Rhat
Density [Site 1]	1.1	1.7	2.7	1.004
Density [Site 2]	1.0	1.6	2.7	1.003
Density [Site 3]	1.1	1.7	2.8	1.008
Density [Site 4]	1.1	1.8	2.9	1.001
Density [Site 5]	1.0	1.6	2.5	1.004
P_{ID}	0.34	0.65	0.95	1.001
sd.cam	0.116	0.509	0.975	1.035
sd.dayCAM	0.116	0.509	0.975	1.035
sd.diver	0.116	0.509	0.975	1.035
sd.dayUVC	0.026	0.105	0.383	1.001

3.2. Simulation data

The relevance of taking into account P_{ID} when estimating fish density using RUV data only is clearly demonstrated with the results obtained from the 4 simulations, because precision and accuracy of the estimated densities can be compared with the true (simulated) fish density, which was 0.016 fish m^{-2} (Section 3.1).

Simulation 1 emulated the case in which any fish within the area surveyed by the camera in a given frame is detected and counted ($P_{ID.sim}$ = 1 and $P_{ID.model}$ = 1; Fig. 3a–e). As expected, the estimated fish densities in that case were very accurate after a relatively small sampling effort (Fig. 3). After 73 frames, i.e. the number of frames used in the fieldwork, the average density (from 100 replicates) was 0.017 (interquartile range [IQR]: 0.015–0.018). Moreover, precision was excellent. For example, in a given replicate (a set of 10 cameras), the 95% Bayesian credibility interval (BCI) was between 0.013 and 0.021, which included the true value (0.016 ind. m^{-2}) in all 100 replicates.

Simulation 2 emulated the case in which only an average of 65% of the fish that are actually within the area surveyed by the camera in a given frame are actually counted ($P_{ID.sim}$ = 0.65), but this imperfect detection is ignored when estimating fish density from those counts ($P_{ID.model}$ = 1; Fig. 3b–f). As expected, fish density was underestimated, and the size of the bias was around 35% (i.e. 1 – $P_{ID.sim}$). After 73 frames, the average density (from 100 replicates) was 0.011 (IQR: 0.010–0.012). In this case, precision was excellent, but the estimates were biased even after increasing the sampling effort in terms of the number of frames included in the analyses. For example, in a given replicate (a set of 10 cameras), the 95% BCI was between 0.008 and 0.015. Moreover, the 95% BCI included the true value (0.016 ind. m^{-2}) in only the 24% of the 100 replicates.

Simulation 3 emulated the case in which only an average of 65% of the fish that are actually within the area surveyed by the camera are counted ($P_{ID.sim}$ = 0.65; Fig. 3c–g). However, and contrary to Simulation 2, in this case it is assumed that $P_{ID.model}$ has been previously estimated using the protocol described in Sections 2.2 and 2.3. This value of $P_{ID.model}$ was included as input when estimating fish density. In that case, the estimated fish density was no longer biased as in Simulation 2, but was accurate. After 73 frames, the average density (from 100 replicates) was 0.017 (IQR: 0.015–0.018), very similar to the values obtained in Simulation 1. Similarly, precision was excellent; for example, in a given replicate (a set of 10 cameras), the 95% BCI was between 0.012 and 0.023 and included the true value (0.016 ind. m^{-2}) in all 100 replicates.

Finally, Simulation 4 was very similar to Simulation 3. The unique difference in Simulation 4 is that the uncertainty in $P_{ID.model}$ has been accounted for (Fig. 3d–h). In that case, the estimated fish density was accurate, but the uncertainty in $P_{ID.model}$ translated into worse precision estimates for fish density. After 73 frames, the average density (from 100 replicates) was 0.017 (IQR: 0.015–0.018), very similar to those obtained in Simulations 1 and 3. Simultaneously, precision was not as good as in Simulation 3; in this case, the precision was wider. For example, in a given replicate (a set of 10 cameras), the 95% BCI was between 0.010 and 0.047 and included the true value (0.016 ind. m^{-2}) in all 100 replicates.

Note that this is the more realistic simulation set. In fact, we strongly suggest completing a similar simulation exercise in order to assess the sampling effort in terms of cameras and deployment time needed to achieve a target precision with the values of density and P_{ID} estimated in a previous pilot study. To facilitate such exercises, the script used for the simulations and the easy-to-use Shiny app are available at https://fishecology.shinyapps.io/uvccam/ (accessed 20 Dec 2018).

For completeness, a sensitivity analysis was carried out with different detectabilities and different densities to assess how these variables affected the accuracy and precision of RUV-only estimates of fish density. The sensitivity analysis showed that when the density of individuals in the environment and the P_{ID} increase, the effort (in number of frames) needed to extract the real density using RUV decreases. In addition, from detectabilities close to 25%, it is possible to obtain the density of animals with a relatively low effort (in number of frames), even when the real density in the environment is low (0.01 ind. m^{-2}) (Fig. S3).

4. DISCUSSION

We have successfully demonstrated a new framework that combines UVC and RUV for the concurrent estimation of fish density (individuals per unit area) and P_{ID}. The estimated fish density of *Serranus scriba* on the SW coast of Mallorca (0.016 ind. m^{-2}; 95% BCI: 0.011–0.027) is within the range reported using other methods at other sites in Mallorca (Deudero et al. 2008) or in the Western Mediterranean (García-

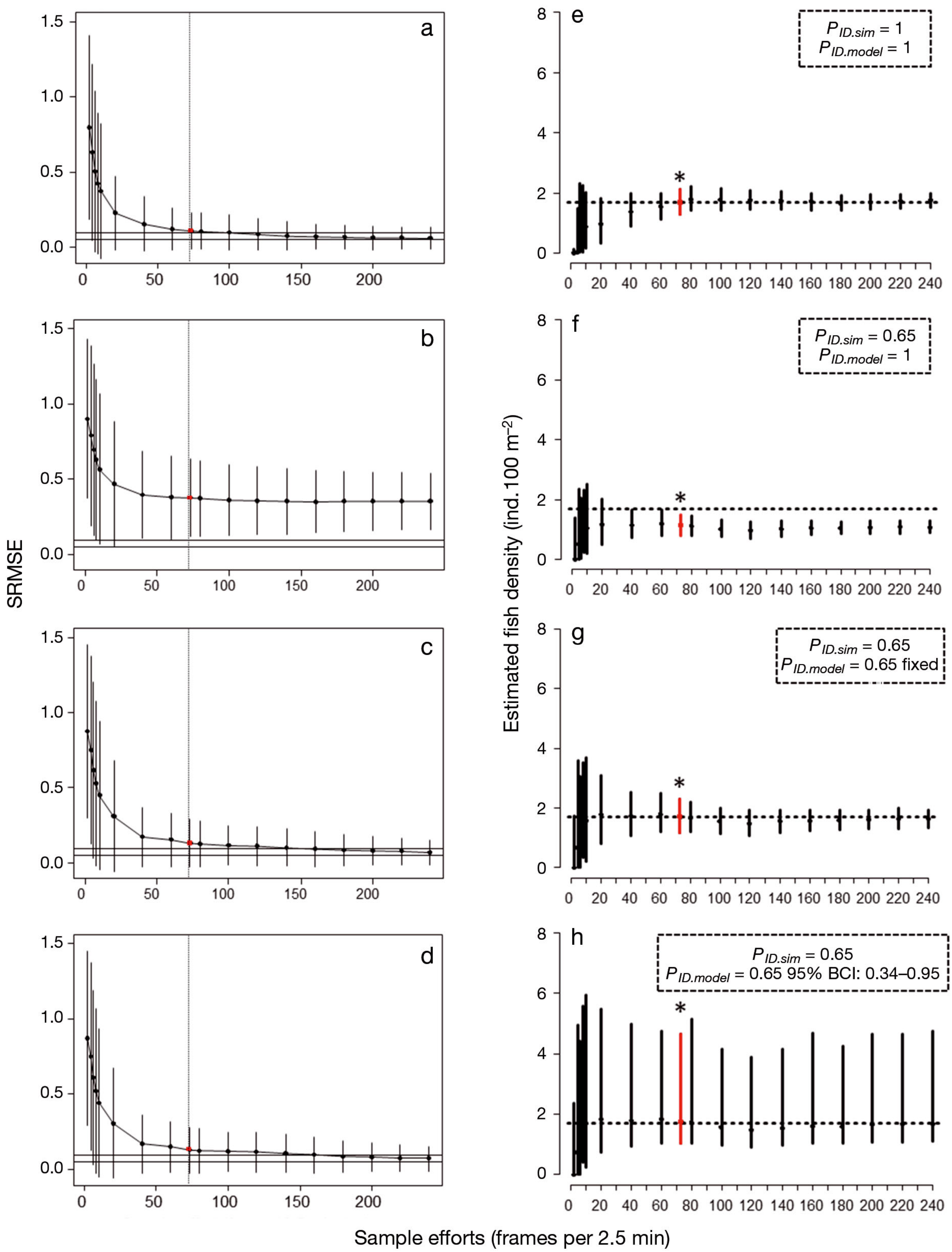

Fig. 3. Results from simulations 1 to 4 (see Section 2.4 for details), showing (a–d) scaled root mean squared error (SRMSE), which represents the accuracy of density estimates (*y*-axis). The *x*-axis shows the increasing effort in the number of frames (frames analysed by 10 cameras). The continuous horizontal lines correspond to threshold values of 10 and 5% of the SRMSE. (e–h) Precision of the estimated density with increasing sampling effort. Black points are mean values with 95% Bayesian credibility intervals (BCI) of the medians from posterior distributions of the density estimates for 10 cameras. The horizontal dotted lines correspond to the true density value obtained from empirical data combining underwater visual census (UVC) and remote underwater video (RUV). The asterisks (with red dot and line) indicate the effort, in frames, used in the fieldwork. Insets describe the individual detectability used in each simulation ($P_{ID.sim}$) and analysis ($P_{ID.model}$)

Charton & Pérez-Ruzafa 2001, Arechavala-López et al. 2008).

The results from our case study prove the opportunities afforded by our method with the possibility of estimating P_{ID}. As mentioned above, the relevance of the proposed framework is that after estimating P_{ID}, fish density can be estimated accurately and precisely at the scale of the preferred reference method using only RUV. Thus, provided that none of the commonly used reference methods for estimating density of resident coastal fish is precise enough, the possibility of an extensive use of properly calibrated RUV may contribute to substantially enlarge the spatio-temporal scope of density monitoring programmes for many resident coastal fish species.

UVC is one of the most common methods used by scientists, managers and stakeholders for estimating the density of many species of coastal fish. The pros and cons of UVC have been comprehensively outlined above, but here we emphasize that the cost in terms of time and effort precludes large sample sizes, and thus densities are usually estimated with wide confidence intervals; as a result, ecologically relevant processes may remain undetected. The costs of RUV deployment are often misperceived as being similar or even larger, especially when including video post processing (Murphy & Jenkins 2010, Pita et al. 2014). However, the cost per sample is by far more cost-effective. Moreover, recent advances in machine learning foresee cost reduction after developing applications for unsupervised recognition of fish from videos (Boom et al. 2014, Hsiao et al. 2014, Sun et al. 2018). The major problem of RUV is that, in general, not all of the fish that are actually within the area surveyed by the camera are detected (i.e. P_{ID} tends to be less than 100%), thus fish density tends to be underestimated in relation to the preferred reference method.

Combining the advantages of UVC and RUV is certainly appealing. The need for combining data gathered using different methods has been repeatedly reported. Specifically, simultaneous use of RUV and UVC has been extensively advised (Willis et al. 2000, Cappo et al. 2003, Stobart et al. 2007, Murphy & Jenkins 2010, Harvey et al. 2013, Shortis et al. 2013, Bacheler et al. 2017, Bosch et al. 2017). However, in most of those cases, the results obtained using different methods are not combined but are only compared (Cappo et al. 2004, Assis et al. 2013, Tessier et al. 2013, Mallet et al. 2014, Pita et al. 2014, Bacheler et al. 2017). Conversely, the framework proposed here offers the possibility for a genuine combination of fish counts using RUV with fish counts obtained by some other reference method, to provide a more realistic view of the fish densities in coastal areas. Moreover, the Bayesian approach proposed here could be easily adapted to the specificities of any sampling strategy (e.g. including the confounding effects of covariables or different levels of random factors, such as between-day or between-camera effects), and our simulation tool-kit allows for extensive pre-sampling for selection of optimal settings (e.g. number of cameras and recording time).

We are not only proposing to combine RUVs with the preferred reference method to improve the precision of the estimated density at any new site or time. While this may be an alternative in some cases, we propose going one step further. Firstly, we suggest concurrently conducting RUVs and UVCs in a single or in a few preliminary experiments to estimate P_{ID} (following the protocol detailed in Sections 2.2 and 2.3). Secondly, after such a calibration exercise, we suggest deploying a large number of cameras to estimate density at several sites and time points to cover large spatial and temporal scales. According to the simulation experiments reported here, this might be a reliable alternative. Note that the need for intercalibration exercises has been repeatedly advised when comparing different methods of underwater camera surveys (Watson et al. 2005) or when suggesting that fish counts during a given UVC should be made by more than one scuba diver at the same time (Bernard et al. 2013). However, the framework proposed here has a broader applicability. The extensive simulation experiments completed here suggest that density estimates may be accurate even when P_{ID} is relatively small or even when it has been inaccurately estimated (Fig. S3). Indeed, in the latter case (Fig. 3), the sampling effort must be larger to attain a target precision, and the question of how to optimally enlarge the sampling effort is an elusive topic. We strongly suggest completing a pilot experiment to identify the levels of larger variability. For example, in the case study reported here, the large between-camera variance suggests the existence of heterogeneous habitats at the within-site level, thus making it advisable to increase the number of cameras per site and perhaps to reduce the number of frames surveyed per camera. This could be achieved either by reducing the deployment time or by enlarging the time between 2 consecutive frames. The sensitivity analyses (Fig. S3) report the main patterns expected after changes in fish density and detectability, and estimate the expected cost (in terms of sampling effort) needed to achieve a target precision. Moreover, the R scripts and the Shiny app provided here may help determine the optimal allocation of sampling effort for any given case.

Some specificities of the case study here deserve special attention. *S. scriba* moves relatively slowly within the area surveyed by the divers, thus, it is reasonable to assume that UVCs were synoptic in the sense that no fish entered or exited the area surveyed during the sampling period (Ward-Paige et al. 2010). Moreover, in our case, UVCs were specifically designed for counting *S. scriba* only, and special care was invested in searching within cavities and seagrass patches. Under these or similar specific circumstances, it may be feasible to assume that UVCs detect close to 100% of the individuals. In those specific cases, fish counts from RUVs only, and after calibrating for P_{ID}, will render absolute density (fish m^{-2}), as indicated in Eq. (4).

Note also that the BCI for P_{ID} in the study case here is wide (0.34–0.95). Imprecise estimation of P_{ID} translates into imprecise density estimates, thus, there is still room for many improvements. Increasing sampling effort when calibrating P_{ID} would certainly increase P_{ID} precision. This may be achieved by increasing the number of UVCs (or the area surveyed), by increasing the number of RUVs, the deployment time, the number of frames analysed by each camera or the area surveyed by the camera. In addition, some improvements concerning the RUV design may be advantageous. For example, when RUVs view parallel to the sea bottom (as those used in the experiments completed here), some fish may remain hidden behind a rock or a vegetation patch, which increases uncertainty. Conversely, RUVs looking down toward the bottom may improve not only P_{ID} but also its precision.

A number of variables may affect P_{ID} and should be accounted for. First, cryptic species should not be considered as optimal candidates for the framework reported here. Moreover, detectability of the same individual may be habitat-dependent (complexity of the bottom structure). Seasonal differences in fish behaviour (i.e. fish may be more active and thus be more easily detected in warmer seasons), any other behaviour specificity or even fish size may affect detectability. Therefore, it is mandatory to take into account the behavioural attributes of the species studied prior to selecting a specific UVC and/or RUV design (Cheal & Thompson 1997, Samoilys & Carlos 2000, Ward-Paige et al. 2010). Provided that the area surveyed by the camera is small, it should also be environmentally homogeneous. However, in UVCs, unaccounted sea bottom heterogeneity within a given transect is expected to increase the unaccounted variance in fish counts, which will translate to P_{ID}. Thus, many small but environmentally homogeneous UVCs would be preferred against a few large but heterogeneous UVCs (Murphy & Jenkins 2010). As mentioned above, UVCs should be as synoptic as possible, which ultimately depends on both fish and diver speed (Ward-Paige et al. 2010, Pais & Cabral 2017). The design of RUVs and UVCs should be carefully selected to minimize all potential confounding effects mentioned above. Moreover, habitat-specific P_{ID} or similar dependencies can be empirically estimated after carefully designed calibration experiments.

Therefore, after solving these case-specific challenges, the methodological framework proposed here suggests that RUV surveys might be included in the basic tool-kit in order to produce more reliable abundance estimates, thus enabling improvements in the management of coastal fish populations.

Acknowledgements. G.F.-B. and C.D.-G. were supported by a PhD fellowship (FPI-INIA) from the National Institute for Agricultural and Food Research and Technology (INIA). A.C.-C was supported by a Spanish FPU PhD fellowship (ref. FPU13/01440). P.A.-L. and J.A. were supported by Juan de la Cierva Incorporación postdoctoral grants (refs. IJCI-2015-25595 and IJCI-2016-27681, respectively). This work was funded by R+D project PHENOFISH (ref. CTM2015-69126-C2-1-R; MINECO) and is a contribution of the Joint Research Unit IMEDEA-LIMIA. This study was carried out with permission from the fisheries local administration, Government of the Balearic Islands. We also thank the researchers and students involved in the fieldwork.

LITERATURE CITED

Ackerman JL, Bellwood DR (2000) Reef fish assemblages: a re-evaluation using enclosed rotenone stations. Mar Ecol Prog Ser 206:227–237

Agnew DJ, Gutiérrez NL, Butterworth DS (2013) Fish catch data: less than what meets the eye. Mar Policy 42: 268–269

Aguzzi J, Doya C, Tecchio S, De Leo FC and others (2015) Coastal observatories for monitoring of fish behaviour and their responses to environmental changes. Rev Fish Biol Fish 25:463–483

Alós J, Palmer M, Catalan IA, Alonso-Fernández A and others (2014) Selective exploitation of spatially structured coastal fish populations by recreational anglers may lead to evolutionary downsizing of adults. Mar Ecol Prog Ser 503:219–233

Alós J, Palmer M, Trías P, Díaz-Gil C, Arlinghaus R (2015) Recreational angling intensity correlates with alteration of vulnerability to fishing in a carnivorous coastal fish species. Can J Fish Aquat Sci 72:217–225

Alós J, Palmer M, Balle S, Arlinghaus R (2016) Bayesian state-space modelling of conventional acoustic tracking provides accurate descriptors of home range behavior

in a small-bodied coastal fish species. PLOS ONE 11: e0154089
Alós J, Campos-Candela A, Arlinghaus R (2018) A modelling approach to evaluate the impact of fish spatial behavioural types on fisheries stock assessment. ICES J Mar Sci 76:489–500
Arechavala-López P, Bayle-Sempere J, Sánchez-Jerez P, Valle C and others (2008) Biodiversity and structure of rocky reef fish assemblages in the Sierra Helada Natural Park (South-western Mediterranean Sea). Arxius Misc Zool 6:232–254
Assis J, Claro B, Ramos A, Boavida J, Serrão EA (2013) Performing fish counts with a wide-angle camera, a promising approach reducing divers' limitations. J Exp Mar Biol Ecol 445:93–98
Bacheler NM, Geraldi NR, Burton ML, Muñoz RC, Kellison GT (2017) Comparing relative abundance, lengths, and habitat of temperate reef fishes using simultaneous underwater visual census, video, and trap sampling. Mar Ecol Prog Ser 574:141–155
Bayley PB, Peterson JT (2001) An approach to estimate probability of presence and richness of fish species. Trans Am Fish Soc 130:620–633
Bernard ATF, Götz A, Kerwath SE, Wilke CG (2013) Observer bias and detection probability in underwater visual census of fish assemblages measured with independent double-observers. J Exp Mar Biol Ecol 443: 75–84
Boom BJ, He J, Palazzo S, Huang PX and others (2014) A research tool for long-term and continuous analysis of fish assemblage in coral-reefs using underwater camera footage. Ecol Inform 23:83–97
Bosch NE, Gonçalves JMS, Erzini K, Tuya F (2017) 'How' and 'what' matters: sampling method affects biodiversity estimates of reef fishes. Ecol Evol 7:4891–4906.
Boulinier T, Nichols JD, Sauer JR, Hines JE, Pollock KH (1998) Estimating species richness: the importance of heterogeneity in species detectability. Ecology 79:1018–1028
Campbell MD, Pollack AG, Gledhill CT, Switzer TS, DeVriese DA (2015) Comparison of relative abundance indices calculated from two methods of generating video count data. Fish Res 170:125–133
Campos-Candela A, Palmer M, Balle S, Alós J (2018) A camera-based method for estimating absolute density in animals displaying home range behaviour. J Anim Ecol 87: 825–837
Cappo M, Harvey E, Malcolm H, Speare P (2003) Potential of video techniques to monitor diversity, abundance and size of fish in studies of marine protected areas. In: Beumer JP, Grant A, Smith DC (eds) Aquatic protected areas. What works best and how do we know? Australian Society for Fish Biology, North Beach, p 455–464
Cappo M, Speare P, De'Ath G (2004) Comparison of baited remote underwater video stations (BRUVS) and prawn (shrimp) trawls for assessments of fish biodiversity in inter-reefal areas of the Great Barrier Reef Marine Park. J Exp Mar Biol Ecol 302:123–152
Cheal AJ, Thompson AA (1997) Comparing visual counts of coral reef fish: implications of transect width and species selection. Mar Ecol Prog Ser 158:241–248
Deudero S, Morey G, Frau A, Moranta J, Moreno I (2008) Temporal trends of littoral fishes at deep *Posidonia oceanica* seagrass meadows in a temperate coastal zone. J Mar Syst 70:182–195
Díaz-Gil C, Smee SL, Cotgrove L, Follana-Berná G and others (2017) Using stereoscopic video cameras to evaluate seagrass meadows nursery function in the Mediterranean. Mar Biol 164:137
Dickens LC, Goatley GHR, Tanner JK, Bellwood DR (2011) Quantifying relative diver effects in underwater visual censuses. PLOS ONE 6:e18965
Dorazio RM, Royle JA (2005) Estimating size and composition of biological communities by modeling the occurrence of species. J Am Stat Assoc 100:389–398
Dunlop KM, Ruxton GD, Scott EM, Bailey DM (2015) Absolute abundance estimates from shallow water baited underwater camera surveys; a stochastic modelling approach tested against field data. Ecology 472:126–134
Easton RR, Heppell SS, Hannah RW (2015) Quantification of habitat and community relationships among nearshore temperate fishes through analysis of drop camera video. Mar Coast Fish 7:87–102
García-Charton JA, Pérez-Ruzafa Á (2001) Spatial pattern and the habitat structure of a Mediterranean rocky reef fish local assemblage. Mar Biol 138:917–934
Hilborn R, Walters CJ (1992) Quantitative fisheries stock assessment: choice, dynamics and uncertainty. Springer, Dordrecht
Hsiao YH, Chen CC, Lin SI, Lin FP (2014) Real-world underwater fish recognition and identification, using sparse representation. Ecol Inform 23:13–21
Kulbicki M, Cornuet N, Vigliola L, Wantiez L, Mou-Tham G, Chabanet P (2010) Counting coral reef fishes: interaction between fish life-history traits and transect design. J Exp Mar Biol Ecol 387:15–23
Lennox RJ, Alós J, Arlinghaus R, Horodysky A, Klefoth T, Monk CT, Cooke SJ (2017) What makes fish vulnerable to capture by hooks? A conceptual framework and a review of key determinants. Fish Fish 18:986–1010
Lindfield SJ, Harvey ES, McIlwain J, Halford (2014) Silent fish surveys: bubble-free diving highlights inaccuracies associated with SCUBA-based surveys in heavily fished areas. Methods Ecol Evol 5:1061–1069
Mallet D, Wantiez L, Lemouellic S, Vigliola L, Pelletier D (2014) Complementarity of rotating video and underwater visual census for assessing species richness, frequency and density of reef fish on coral reef slopes. PLOS ONE 9:
Mallet D, Pelletier D (2014) Underwater video techniques for observing coastal marine biodiversity: a review of sixty years of publications (1952–2012). Fish Res 154: 44–62
March D, Palmer M, Alós J, Grau A, Cardona F (2010) Short-term residence, home range size and diel patterns of the painted comber *Serranus scriba* in a temperate marine reserve. Mar Ecol Prog Ser 400:195–206
Murphy HM, Jenkins GP (2010) Observational methods used in marine spatial monitoring of fishes and associated habitats: a review. Mar Freshw Res 61:236–252
Ordines F, Moranta J, Palmer M, Lerycke A, Suau A, Morales-Nin B, Grau AM (2005) Variations in a shallow rocky reef fish community at different spatial scales in the western Mediterranean Sea. Mar Ecol Prog Ser 304: 221–233
Pais MP, Cabral HN (2017) Fish behaviour effects on the accuracy and precision of underwater visual census surveys. A virtual ecologist approach using an individual-based model. Ecol Model 346:58–69
Palmer M, Balle S, March D, Alós J, Linde M (2011) Size

estimation of circular home range from fish mark-release-(single)-recapture data: case study of a small labrid targeted by recreational fishing. Mar Ecol Prog Ser 430:87–97
Pauly D, Hilborn R, Branch TA (2013) Fisheries: Does catch reflect abundance? Nature 494:303–306
Pelletier D, Leleu K, Mallet D, Mou-Tham G, Hervé G, Boureau M, Guilpart N (2012) Remote high-definition rotating video enables fast spatial survey of marine underwater macrofauna and habitats. PLOS ONE 7: e30536
Pita P, Villasante S, Arlinghaus R, Gomes P and others (2018) A matter of scales: Does the management of marine recreational fisheries follow the ecosystem approach to fisheries in Europe? Mar Policy 97:61–71
Pita P, Fernández-Márquez D, Freire J (2014) Short-term performance of three underwater sampling techniques for assessing differences in the absolute abundances and in the inventories of the coastal fish communities of the Northeast Atlantic Ocean. Mar Freshw Res 65:105–113
Plummer M, Best N, Cowles K, Vines K (2006) CODA: convergence diagnosis and output analysis for MCMC. R News 6:7–11
Plummer M (2015) JAGS Version 4.0.0 user manual. http://mcmc-jags.sourceforge.net/
Przeslawski R, Foster SD (2018) Field manuals for marine sampling to monitor Australian waters. http://pid.geoscience.gov.au/dataset/ga/115821
R Core Team (2017) R: a language and environment for statistical computing. R Foundation for Statistical Computing, Vienna
Samoilys MA, Carlos G (2000) Determining methods of underwater visual census for estimating the abundance of coral reef fishes. Environ Biol Fishes 57:289–304
Schobernd ZH, Bacheler NM, Conn PB (2014) Examining the utility of alternative video monitoring metrics for indexing reef fish abundance. Can J Fish Aquat Sci 71: 464–471
Shortis MR, Ravanbakskh M, Shaifat F, Harvey ES and others (2013) A review of techniques for the identification and measurement of fish in underwater stereo-video image sequences. Proc SPIE 8791, Videometrics, Range Imaging, and Applications XII; and Automated Visual Inspection, Munich, 87910G
Stobart B, García-Charton JA, Espejo C, Rochel E and others (2007) A baited underwater video technique to assess shallow-water Mediterranean fish assemblages: methodological evaluation. J Exp Mar Biol Ecol 345:158–174
Stobart B, Díaz D, Álvarez F, Alonso C, Mallol S, Goñi R (2015) Performance of baited underwater video: Does it underestimate abundance at high population densities? PLOS ONE 10:e0127559
Struthers DP, Danylchuk AJ, Wilson ADM, Cooke SJ (2015) Action cameras: bringing aquatic and fisheries research into view. Fisheries 40:502–512.
Su YS, Yajima M (2015) R2jags: using R to run 'JAGS'. R package version 0.5-7. CRAN.R-project.org/package=R2jags (September 2015)
Sun X, Shi J, Liu L, Dong J, Plant C, Wang X, Zhou H (2018) Transferring deep knowledge for object recognition in low-quality underwater videos. Neurocomputing 275: 897–908
Tessier A, Pastor J, Francour P, Saragoni G, Crec'hriou R, Lenfant P (2013) Video transects as a complement to underwater visual census to study reserve effect on fish assemblages. Aquat Biol 18:229–241
Thompson AA, Mapstone BD (1997) Observer effects and training in underwater visual surveys of reef fishes. Mar Ecol Prog Ser 154:53–63
Villegas-Ríos D, Alós J, Palmer M, Lowerre-Barbieri SK, Bañón R, Alonso-Fernández A, Saborido-Rey F (2014) Life-history and activity shape catchability in a sedentary fish. Mar Ecol Prog Ser 515:239–250
Walther BA, Moore JL (2005) The concepts of bias, precision and accuracy, and their use in testing the performance of species richness estimators, with a literature review of estimator performance. Ecography 28:815–829
Ward-Paige C, Mills Flemming J, Lotze HK (2010) Overestimating fish counts by non-instantaneous visual censuses: consequences for population and community descriptions. PLOS ONE 5:e11722
Watson DL, Harvey ES, Anderson MJ, Kendrick GA (2005) A comparison of temperate reef fish assemblages recorded by three underwater stereo-video techniques. Mar Biol 148:415–425
Whitmarsh SK, Fairweather PG, Huveneers C (2017) What is Big BRUVver up to? Methods and uses of baited underwater video. Rev Fish Biol Fish 27:53–73
Willis TJ, Millar RB, Babcock RC (2000) Detection of spatial variability in relative density of fishes: comparison of visual census, angling, and baited underwater video. Mar Ecol Prog Ser 198:249–260

Editorial responsibility: Lisandro Benedetti-Cecchi, Pisa, Italy

Submitted: July 10, 2018; Accepted: March 6, 2019
Proofs received from author(s): April 15, 2018